Heat and Mass Transfer 34 (1998) 263–270 © Springer-Verlag 1998

Mixed convection heat transfer in open ended channels with protruding heaters

S-Q. Du, E. Bilgen, P. Vasseur

Abstract Mixed convection heat transfer has been studied in vertical channels, open at the bottom and top, with protruding discrete heaters installed on one side. The flow is assumed to be steady, laminar and two-dimensional. The Boussinesq approximation is used to account for the density variation. Non-dimensional equations of conservation of mass, momentum and energy, with the Boussinesq approximation are solved using the SIMPLER method. Heat transfer through the top and the right are calculated as functions of the Rayleigh number ($0 \leq \mathrm{Ra} \leq 10^7$), the Reynolds number ($0 \leq \mathrm{Re} \leq 200$), various aspect ratios ($1 \leq A \leq 6$). The effect of the entrance and exit lengths and that of the position of the electronic components in the channel are also examined. Flow and temperature fields for various cases are produced, and the temperature variations in the electronic components are calculated.

List of symbols

A	enclosure aspect ration, H/L
c_p	heat capacity, J/kg · K
g	acceleration due to gravity, m/s^2
h	electronic component height, m
H	channel height, m
k	thermal conductivity, W/m · K
L	channel width, m
ℓ	electronic component thickness, m
Nu	Nusselt number = hL/k
p	pressure, Pa
P	dimensionless pressure, = $(p - p_0)/\rho v_0^2$
Pr	prandtl number = v/α
Q	heat transfer, total heat transfer = $S\Sigma v_{\mathrm{chips}}$, W
Ra	Rayleigh number = $g\beta\Delta T_{\max} L^3/(v\alpha)$
Re	Reynolds number = $v_0 L/v$
R_k	conductivity ratio = k_s/k_f
S	volumetric heat source, W/m^3
T	temperature, K
U, V	dimensionless fluid velocities, = $u/v_0, v/v_0$
v_{chips}	volume of the chips, m^3
X, Y	dimensionless distance on x and y, = $x/L, y/L$

Greek letters

β	thermal expansion of fluid, 1/K
$\Delta T_{\max}$	maximum temperature difference, = SL^2/k
v	kinematic viscosity, m^2/s
ρ	fluid density, kg/m^3
θ	dimensionless temperature, = $(T - T_0)/\Delta T_{\max}$

Subscript

B	bottom of the channel
f	fluid
$_L$	left boundary of the channel
R	right boundary of the channel
S	solid
T	top of the channel
$_0$	entrance
$_{1,2,3}$	first, second and third electronic component
$_{01,02,03}$	distances from entrance to first component, from first to second and from second to third respectively

Superscript

$^-$	average

1 Introduction

The high packaging density and the increasing heat fluxes have significantly changed the role of cooling in electronic industries. Since proper cooling is essential yet constrained by acoustic requirements, natural and mixed convection cooling has recently received an increasing attention because of its quieter and more reliable operation. The electronic components are often mounted on PCB boards. Several of these boards may be put together in a cabinet. Here, they form parallel channels containing electronic components, often cooled by forced and buoyancy driven flows [1]. The electronic cabinets contain several PCB boards making repetitive channels, open at the bottom and top. It would be of interest to isolate and study the cooling problem in one channel containing electronic components in which the processes are complicated by the presence of the components and flow separations may exist [2]. The forced flow in these channels is still laminar due to small dimensions and low velocities employed and heat transfer coefficients are characteristically low [3]. A review of the existing literature shows that the recent studies for natural and mixed

Received on 2 March 1998

S-Q. Du, E. Bilgen, P. Vasseur
Department of Mechanical Engineering, École Polytechnique, University of Montreal,
C.P. 6079 Centre Ville, Montreal, Pc, Canada, H3C 3A7

Correspondence to: E. Bilgen

convection in the vertical channels have been widely undertaken both experimentally and by means of numerical analysis (see, for example, [4,5]). Laminar mixed convection between vertical plates with isolated thermal sources has been investigated in which two finite thermal sources located in one of the adiabatic walls and fully developed flow at the channel exit were considered [6]. They found that the heat transfer coefficient for the upper heater is affected by the lower heater, velocities induced by the lower heater enhance the heat transfer from the upper heater. Mixed convection flow over localized multiple thermal sources on a vertical surface has also been investigated [7]. Moreover, the mixed convective heat transfer in vertical cavities with heated bottom surface has been studied by a cubic spline collocation numerical method [8]. A similar problem of laminar natural convection in partially heated vertical channels has been studied for the case of uniform wall temperature or uniform heat flux [9]. The effect of the location of discrete thermal sources on a vertical adiabatic wall was investigated in their study. They found the separation distance between the thermal sources and the ratio of their heat fluxes could affect the heat transfer coefficients. The boundary layer equations for the problem of natural convection in a channel with discrete heating has been also solved [10]. High Rayleigh number laminar natural convection in an asymmetrically heated vertical channel has been studied experimentally [11]. Recently, a numerical study has been carried out on mixed convection heat transfer in inclined open ended channels where isothermal discrete heating elements are equally distanced and placed on one side while isothermal conditions are imposed on the other [12]. They have shown that the normalized Nusselt number was affected considerably by the imposed flow, inclination angle and the strength of the natural convection.

In the above mentioned studies, researches were all concentrated on flush mounted heaters, and relatively few studies have been reported for the protruding components. The aspect ratio effect on natural convection heat transfer in a rectangular enclosure with protruding heat sources has been experimentally investigated [13]. They found that the correlation of the local Nusselt number versus the local modified Rayleigh number was independent of the number of heaters. It has been reported from an experimental study on arrays of small heaters in natural convection that the protruding heaters have higher heat transfer coefficients than the flush mounted ones, indicating the difference between two types of heater [14]. Besides this work, natural convection from block-like heated elements located on a vertical plate has been investigated both experimentally and numerically [2]. The local Nusselt number distributions show that the heat transfer on the upstream side of the heated surface is in general higher than that on the downstream side. The maximum heat flux occurs at the vertical surfaces of the heaters.

The literature review shows that only few studies exist on protruding types of heaters, none on mixed convection in channels with protruding heaters. This case will be undertaken in the present study.

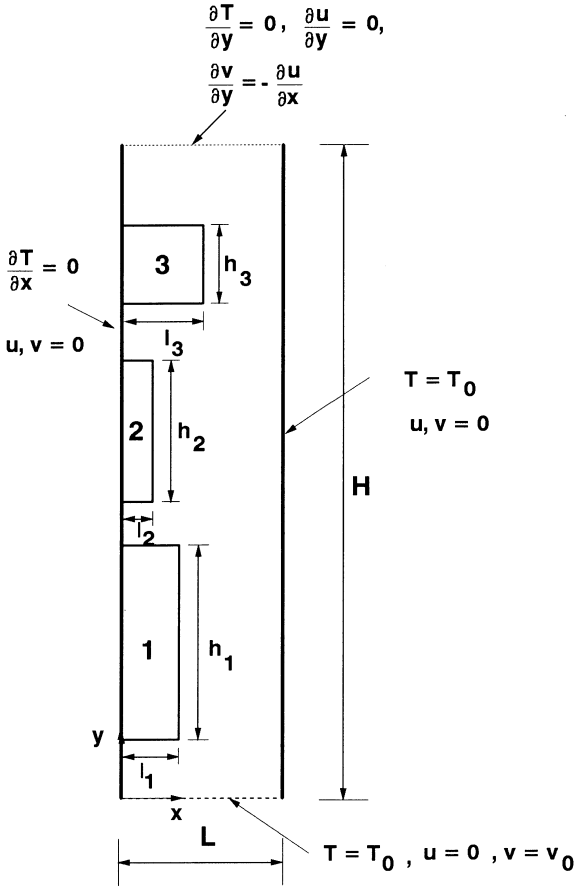

Fig. 1. Schematic of the physical problem, numerical domain and coordinate system

2
System description and mathematical analysis

The schematic of the problem is shown in Fig. 1 where geometry and thermal boundary conditions are given. The system is assumed to have an infinite depth implying that the velocity and temperature distributions depend only on x and y as defined in Fig. 1.

The basic configuration is a two-dimensional vertical channel with height H (6 cm) and width L (1.5 cm). On the left vertical adiabatic surface there are three heated components with different width h and thickness ℓ. The spacing between the heated components is different from one another. The geometrical details will be given later. The heat produced by the electronic components is assumed to be uniformly distributed within the components with an intensity S. Furthermore, the right vertical wall is maintained at a uniform temperature, $T = T_0$. The boundary conditions at the inlet (bottom) and the exit (top) will be defined later.

The flow and heat transfer in a two dimensional laminar natural convection problem of a Newtonian fluid are governed by the continuity, momentum and energy equations according to the coordinate system defined in Fig. 1. The non-dimensional governing equations are

$$\frac{\partial U}{\partial X} + \frac{\partial V}{\partial Y} = 0 \qquad (1)$$

$$U\frac{\partial U}{\partial X}+V\frac{\partial U}{\partial Y}=-\frac{\partial P}{\partial X}+\frac{1}{\mathrm{Re}}\nabla^2 U \tag{2}$$

$$U\frac{\partial V}{\partial X}+V\frac{\partial V}{\partial Y}=-\frac{\partial P}{\partial Y}+\frac{1}{\mathrm{Re}}\nabla^2 V+\frac{\mathrm{Ra}}{\mathrm{Re}^2\mathrm{Pr}}\theta \tag{3}$$

$$U\frac{\partial \theta}{\partial X}+V\frac{\partial \theta}{\partial Y}=\frac{R_k}{\mathrm{RePr}}(\nabla^2\theta+1) \tag{4}$$

where 1 in Eq. (4) comes from the definition of $\Delta T_{\max}$, which is arbitrarily set to 1 for computational purposes. The solid region is characterized with high viscosity and high conductivity, i.e., $R_k = 10^4$, which gives a solid approximation of the medium where U and V approach zero everywhere within the chips. The magnitudes of the velocities using above numerical values were 10^{-9} or smaller. For pure fluid region, $R_k = 1$ and with 1 in the Eq. (4) disappearing, Eqs. (1) to (4) reduce to the Navier-Stokes equations. For the control volume faces coinciding with the chips boundaries, the interface energy balance is automatically satisfied at the fluid-chip interfaces. Boundary conditions are (see Fig. 1):

on solid surfaces	$U = 0,\ V = 0$
on fluid-chip interfaces	$\left(\frac{\partial\theta}{\partial n}\right)_{\mathrm{f}} = R_k\left(\frac{\partial\theta}{\partial n}\right)_{\mathrm{s}}$
on the left wall (on the PCB)	$\frac{\partial\theta}{\partial X}=0$
on the right wall	$\theta = 0$
at the entrance	$U = 0,\ V = 1,\ \theta = 0$
at the exit	$\frac{\partial U}{\partial X}=-\frac{\partial V}{\partial Y}, \frac{\partial U}{\partial Y}=0$ and $\frac{\partial\theta}{\partial Y}=0$

The boundary conditions at the entrance imply that the fluid flow is a developing one and its temperature is equal to the ambient temperature. The boundary conditions at the exit are such that the conservation of mass is satisfied (first condition), i.e., the vertical velocity component is obtained by the mass balance at the boundary cells, the local acceleration across the channel is negligible with respect to that along the channel (second condition) and the heat transfer by conduction at the exit section is negligible with respect to that by convection (third condition). Before carrying out the computations, the last two assumptions were tested by taking various exit lengths and the magnitudes of various terms were examined at various distances from the last electronic component. It was found that for the geometry in Fig. 1, the terms $\frac{\partial U}{\partial Y}$ and $\frac{\partial\theta}{\partial Y}$ at the exit section were indeed negligibly small.

The normalized mean heat transfer at the right, bottom and top boundaries are calculated as

$$Q_{\mathrm{R}}=\frac{\bar{Q}_R}{\bar{Q}}=\frac{1}{A}\int_0^A\left[-\frac{\partial\theta}{\partial X}\right]_{X=1}\mathrm{d}Y \tag{5}$$

$$Q_{\mathrm{B\ or\ T}}=\frac{\bar{Q}_{\mathrm{B\ or\ T}}}{\bar{Q}}=\frac{1}{A}\int_0^1\left[\mathrm{RePr}V\left(\theta+\frac{T_0}{\Delta T_{\max}}\right)-\frac{\partial\theta}{\partial Y}\right]_{Y=0\ \text{or}\ 1}\mathrm{d}X \tag{6}$$

where $\bar{Q}_{\mathrm{T\ or\ B\ or\ R}}$ is the average heat transfer through a section, and $\bar{Q} = kA\Delta T_{\max} = SHL$ is the heat transfer for the case of the electronic components filling the entire channel.

3
Numerical method and computation

The numerical method used to solve Eqs. (1) to (4) is the SIMPLER method [15]. The computer code based on the mathematical formulation discussed earlier and the SIMPLER method are validated for various cases published in the literature, the results of which are discussed elsewhere [16]. Uniform grid was used for all computations. Grid sizes of 12×12, 24×26, 24×32 and 74×74 were tried. Grid independence was achieved within 0.5 percent with a grid size of 24×26 for various channel aspect ratios. It was seen also that the difference of heat transfer through the top, right and bottom with 24×26 and 74×74 was negligible and the streamlines and isotherms were identical. Most of the studies reported in this study were carried out with grid size 24×26. However to see the details of the flow near the chips, some were also carried out with grid size 74×74. The relaxation parameter was varied from 0.11 for $\mathrm{Ra} = 10^5$ to 0.07 for $\mathrm{Ra} = 10^7$. The execution time for a typical case with $A = 4$, the grid size of 24×26, $\mathrm{Ra} = 10^6, \mathrm{Re} \to 0$ and for 287 iterations was 156 C.P.U. seconds on an IBM 3090. For $A = 4$, the same grid size, and $\mathrm{Ra} = 10^6, \mathrm{Re} = 50$ and for 146 iterations it was 100 C.P.U. seconds. The accuracy control was carried out by the conservation of mass by setting its variation to less than 10^{-3}, on the pressure term by setting the variation of residues at 10^{-3}. In addition, the accuracy of computations was checked using the energy conservation within the system, by setting its variation to less than 10^{-4}.

4
Results and discussion

Flow and temperature fields and heat transfer rates are examined for ranges of the Rayleigh number Ra from 10^3 to 10^7, the Reynolds number Re from 10 to 200. The limiting cases with $\mathrm{Ra} \to 0$ corresponding to no natural convection and $\mathrm{Re} \to 0$ corresponding to no forced convection were also studied. All results are for air ($\mathrm{Pr} = 0.72$). First, the results are presented for the channel aspect ratio of $A = 4$ with the geometrical dimensions of the heating components given in Table 1. This is a typical configuration for electronic component design (see, for example, Beckermann and Smith, 1990) and has following dimensionless distances: from the entrance to the first heating component is $h_{01}/L = 0.33$, between the first and second components $h_{02}/L = 0.25$, between the second and third $h_{03}/L = 0.33$ and at the exit $h_e/L = 0.5$. The effect of A, which was varied from 1 to 6 is later examined. The effect of the entrance and exit lengths from the beginning

Table 1. Geometrical configuration for the heating components

Component no.	ℓ/L	h/L	Relative Power
1	1/3	1.25	1.00
2	1/6	0.83	0.33
3	1/2	0.50	0.60

or ending of the electronic components are examined by extending the channel length while keeping the position of the chips the same. The effect of the position of the electronic components with respect to each other is examined by a permutation of the chips 1, 2, 3 (case A; base case) to 1, 3, 2 (case B) and 3, 2, 1 (case C). The heat transfer through the right, top and bottom is calculated by Eqs. (5) and (6) for various Ra and Re numbers. The heat transfer through the left is zero and that through the bottom is usually negligibly small compared to those through the top and right. Hence the heat transfer through the top and right is of interest. Ra is proportional to the heat generated by the electronic components. Hence, the intensity of natural convection increases with increasing Ra. On the other hand, the intensity of the forced convection increases with increasing Re.

The ratio of the heat transfer through the top to the total heat transfer, Q_T/Q, is calculated as a function of Ra and Re and presented in Fig. 2a and b. Here, the total heat transfer is $Q = S\Sigma v_{chips}$, which is also equal to $Q_T + Q_B + Q_R$. Figure 2a shows that the heat transfer through the top is a decreasing function of Ra for low forced convection. This indicates that as the Rayleigh number increases, the natural convection increases, so does the heat transfer through the right boundary. As a result, the heat transfer through the top gradually decreases. With increasing Re numbers, for Re = 100 and 200 in Fig. 2a, the heat transfer is almost entirely through the top and it is independent of Ra. This indicates that the dominant heat transfer mode for these high Re numbers is by forced convection. This mechanism will be discussed later in detail. The heat transfer through the top as a function of Re number with Ra number as a parameter, is shown in Fig. 2b. As expected, for a given Ra number, the heat transfer is an increasing function of Re number and as observed earlier in Fig. 2a, the heat transfer becomes almost entirely through the top for high Re numbers. At low Re numbers, the heat transfer increases with decreasing Ra number, which is, as explained earlier, indicative of increasing heat transfer to the right at increasing Ra numbers.

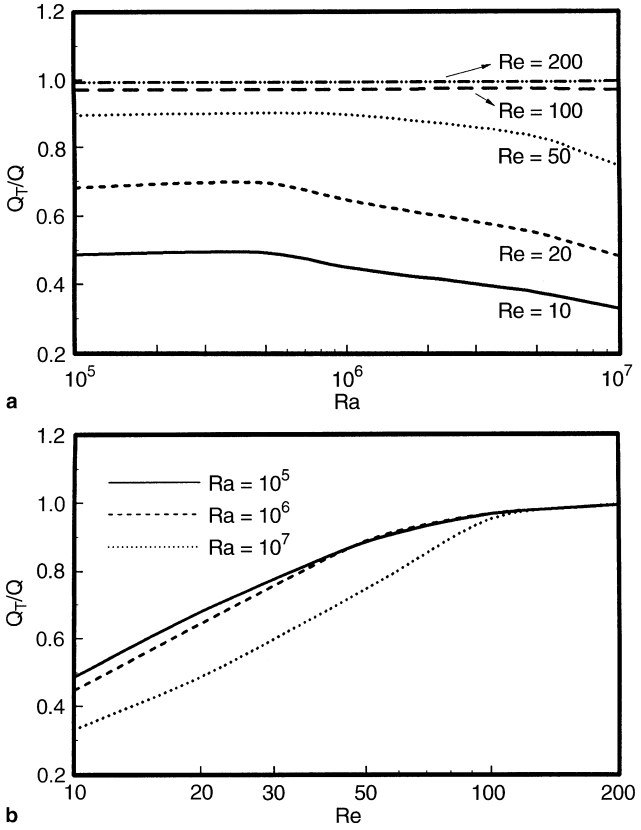

Fig. 2a,b. Heat transfer through the top, Q_T/Q by mixed convection for the base case with $A = 4$. **a** Dimensionless heat transfer through the top, Q_T/Q as a function of the Rayleigh number for various Reynolds numbers. **b** Dimensionless heat transfer through the top, Q_T/Q as function of the Reynolds number for various Rayleigh numbers

The details of the flow and temperature fields for various Re and Ra numbers were studied. The flow fields, for Re = 10 and various Ra numbers, for example, showed (not presented in figures) that the maximum intensity of circulation was $\Psi_{max} = -1.326$ for Ra = 10^5, -3.50 for 10^6 and -6.194 for 10^7. As the circulation increased with increasing Ra number, the interaction between the heaters and the right boundary increased. Hence, the heat transfer through the top decreased as observed earlier in Fig. 2a and b. The temperature fields showed that the isotherms were parallel for Ra = 10^5, indicating a quasi conduction regime. As Ra increased to 10^6, the isotherms showed stratification between the components and the right boundary. At Ra = 10^7, the fluid was completely stratified from the bottom to the top, with high temperature gradients on the electronic components and the right boundary. As Ra increased, the upper two components were surrounded by isotherms at higher temperatures, while the first component stayed at lower temperatures. At Ra = 10^7, all three components were at different temperatures with a strong stratification and the geometrical effect was almost not existing. The maximum dimensionless temperatures were $\theta_{max} = 0.0943$ for Ra = 10^5 at ($X = 0.0208$, $Y = 3.25$), 0.062 for Ra = 10^6 at ($X = 0.0208$, $Y = 3.417$), 0.0413 for Ra = 10^7 at ($X = 0.0208$, $Y = 3.25$). The maximum temperature occurred in the third electronic component for this condition.

The ratio of the heat transfer through the right to the total heat transfer, Q_R/Q, is presented in Fig. 3a and b. It is observed in Fig. 3a that the heat transfer through the right is a slightly increasing function of Ra number especially at low Re numbers. Q_R/Q increases with decreasing Re numbers, indicating that the contribution of the natural convection increases with decreasing forced convection, which is an expected result. Figure 3b shows Q_R/Q as a function of Re number with various Ra numbers as a parameter. Following the observation in Fig. 3a, the heat transfer through the right is a decreasing function of Ra number and a slightly increasing function of Ra number. These results show that at Re $\geq$ 200, the heat transfer through the right becomes less than 1% of the total. As expected, the evacuation of heat from the electronic components is mostly through the top. As the forced convection increases, the heat transfer through the top increases.

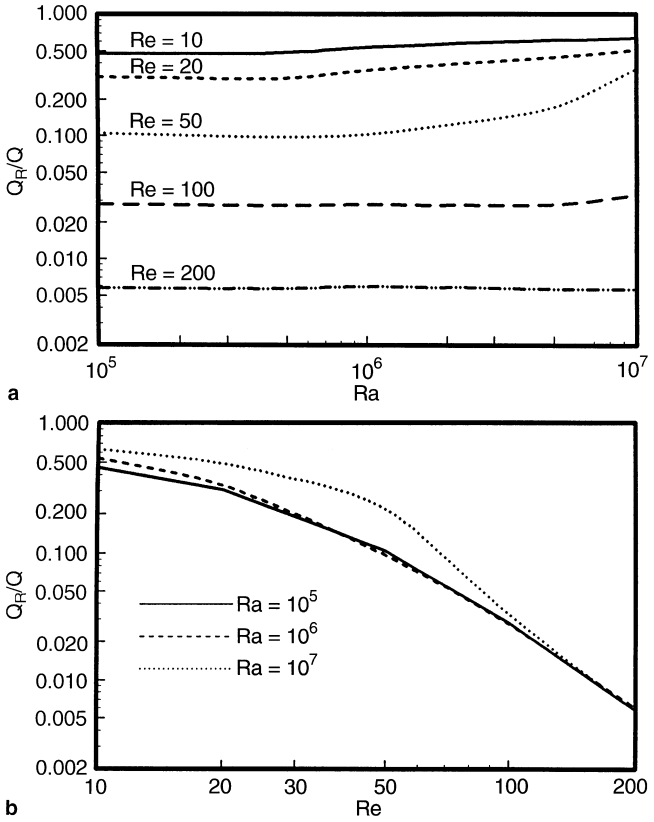

Fig. 3a,b. Heat transfer through the right, Q_R/Q by mixed convection for the base case with $A = 4$. **a** Dimensionless heat transfer through the right, Q_R/Q as a function of the Rayleigh number for various Reynolds numbers. **b** Dimensionless heat transfer through the top, Q_R/Q as function of the Reynolds number for various Rayleigh numbers.

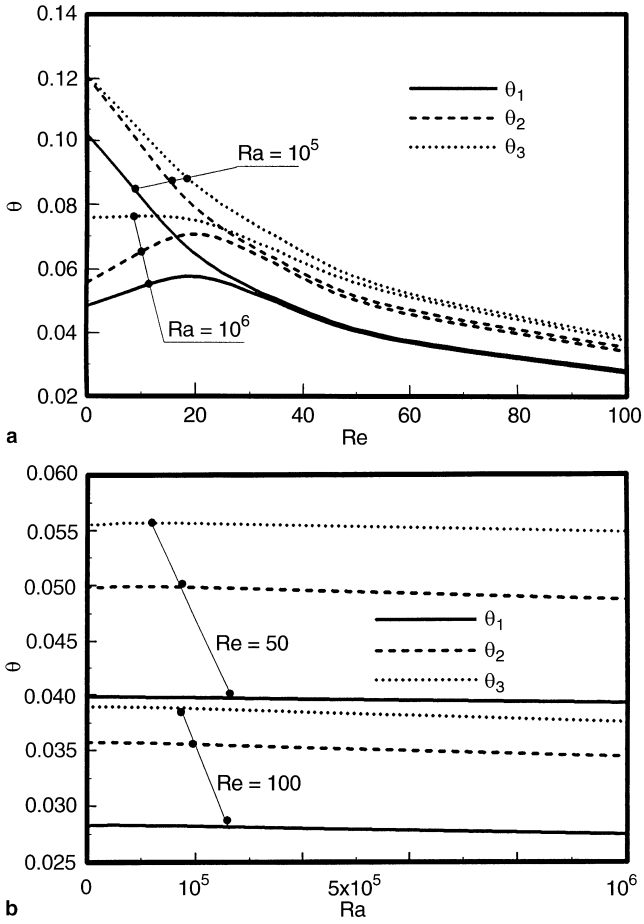

Fig. 4a,b. Temperature at the electronic components as a function of Reynolds and Rayleigh numbers for the base case with $A = 4$. **a** Temperatures θ_i at the electronic components ($i = 1, 2, 3$) as a function of the Reynolds number for $\mathrm{Ra} = 10^5$, **b** Temperatures θ_i at the electronic components ($i = 1, 2, 3$) as a function of the Rayleigh number for $\mathrm{Re} = 50$

The influence and the contribution of the natural convection are felt only when the forced convection is negligibly small and when the heat flux from the electronic components is relatively high. The temperature variation of the electronic components is calculated for various Re and Ra numbers for the base case of $A = 4$. The conductivity of the electronic components being high, the conductivity ratio has an order of magnitude, $R_k = 10^3$ to 10^4. Hence, the results showed that the temperature within each component was almost uniform. The variation of dimensionless temperature as a function of Re number for $\mathrm{Ra} = 10^5$ and 10^6 is shown in Fig. 4a. It is seen that the temperature in the first component is lowest as it is cooled most effectively by incoming air from the bottom of the channel. The second and third components are in the wake of the first component, they are cooled with warmer air, and hence their temperatures are slightly higher. It is also seen that the cooling is generally more effective with increasing Ra number. The temperature is decreasing gradually with increasing Re number for $\mathrm{Ra} = 10^5$ and it is maximum in all three components when $\mathrm{Re} \to 0$, i.e. when there is no forced convection. The situation is different for $\mathrm{Ra} = 10^6$ and the temperature variation shows a maximum at the Reynolds number of about 20 in all three components. To understand the reason for passing from a maximum at $\mathrm{Ra} = 10^6$, the heat transfer through various sections were examined and compared for $\mathrm{Re} \to 0$, $\mathrm{Re} = 20$ and 50. It was seen that for $\mathrm{Re} \to 0$, the heat transfer through the right and the bottom was more effective in comparison with that for $\mathrm{Re} = 20$, and although the heat transfer through the top was enhanced for $\mathrm{Re} = 20$, the overall cooling was better for $\mathrm{Re} \to 0$. It was noticed further that for $\mathrm{Re} \geq 20$, the heat transfer through various sections had similarities for both $\mathrm{Ra} = 10^5$ and 10^6 and various Re numbers. This indicates that more effective heat transfer through the right is responsible for the observed lower temperatures when $\mathrm{Re} \to 0$ and $\mathrm{Re} = 10^6$. It is seen in Fig. 4a that for $\mathrm{Re} \geq 20$ their variations follow the same trend, i.e. they decrease gradually with increasing Re and Ra numbers, confirming the above reasoning. Figure 4b shows the temperature variation as a function of Ra number for $\mathrm{Re} = 50$ and 100 for which the variation is gradual. The same observation made for Fig. 4a applies for the cooling of various components: the electronic components are cooled best in the order they are arranged in the channel and as the Reynolds number increases, the cooling becomes better. It is also seen that cooling by natural convection at high Reynolds numbers has little effect on the temperature in the components.

The effect of the aspect ratio, A, on the heat transfer from the top, Q_T/Q is studied by changing the width of the channel. L, while keeping the position and the geometry of the electronic components the same. The lower limit of A corresponds to the channel where the right wall is positioned at $L = H$. The upper limit is set by the presence of the electronic components and set at $H = 4\ell_3/3$. It was seen (not presented in figures) that when the aspect ratio was 1, i.e. the right wall is far from the electronic components, for both Ra numbers the dimensionless heat transfer from the top increased with increasing Re number and became equal to 1 for $\mathrm{Re} = 100$ for both $\mathrm{Ra} = 10^5$ and 10^6. When the heat transfer was by natural convection only, i.e. for $\mathrm{Re} \to 0$, the heat transfer through the top passed from a maximum for $\mathrm{Ra} = 10^5$; it was seen that for higher Ra numbers, this trend was not visible. Similar maximum was also seen for the case of mixed convection with $\mathrm{Re} = 50$ and $\mathrm{Ra} = 10^5$ and 10^6. The reason for the observed maxima is that for $\mathrm{Ra} = 10^5$, i.e. for low natural convection, and/or $\mathrm{Re} \to 0$, i.e. no forced convection, there was a reverse flow through the bottom. As mentioned earlier, the reverse flow, hence the heat transfer through the bottom is negligible for high Ra and Re numbers. However, at the limiting situations it has the same order of magnitude as the others. The results have shown that the reverse flow, hence the heat transfer through the bottom was lowest for $A = 2$, which makes the heat transfer through the top a maximum at that aspect ratio for low Ra and Re numbers. It was also seen that for $A \geq 2$, as the aspect ratio increased the heat transfer through the top decreased. The reason for this is that the heat transfer by natural convection increases to the right as the channel becomes closer to the electronic components. An examination of the isotherms for various aspect ratios showed that the dimensionless temperature increased with decreasing A, indicating that the cooling of the electronic components was more favorable for larger channels.

The effects of entrance and exit lengths have been studied by taking the base case with $A = 4$ and keeping the positions of the electronic components the same with respect to each other. To study the entrance length effect, the channel length at the beginning is extended from 4 up to 10 while keeping the exit conditions the same. To study the exit length effect, the channel length at the exit is varied while keeping the entrance conditions the same. All the results are for $\mathrm{Ra} = 10^6$ and presented in Figs. 5 and 6. Heat transfer through the top as a function of the aspect ratio is shown in Fig. 5 for various Re numbers. Figure 5a shows that for the case of natural convection the heat transfer through the top increases slightly with increasing entrance length, which is due to chimney effect. Stream lines for this case showed that the circulation at the level of the electronic components decreased with increasing entrance length. Thus, the heat transfer through the top increases with increasing length of entrance. For the case of mixed convection, it is decreasing slightly with increasing entrance length. An examination of the flow and temperature fields showed that the flow was nearer to the right and the gradient of temperature steeper as the entrance length increased. This resulted in more heat transfer to the right, hence a decrease in Q_T/Q. Figure 5b shows that the heat transfer through the top is a decreasing function of the exit length for both natural and mixed convection for the same reason as discussed earlier in case of the entrance length and also due to better heat transfer to the right from the warm air as the heat transfer surface increases with increasing exit length. Figure 5 shows, in fact, that heat generated in the electronic components can be distributed through the top and the right wall by varying the entrance and exit lengths. It is seen that the exit length is a better controlling parameter.

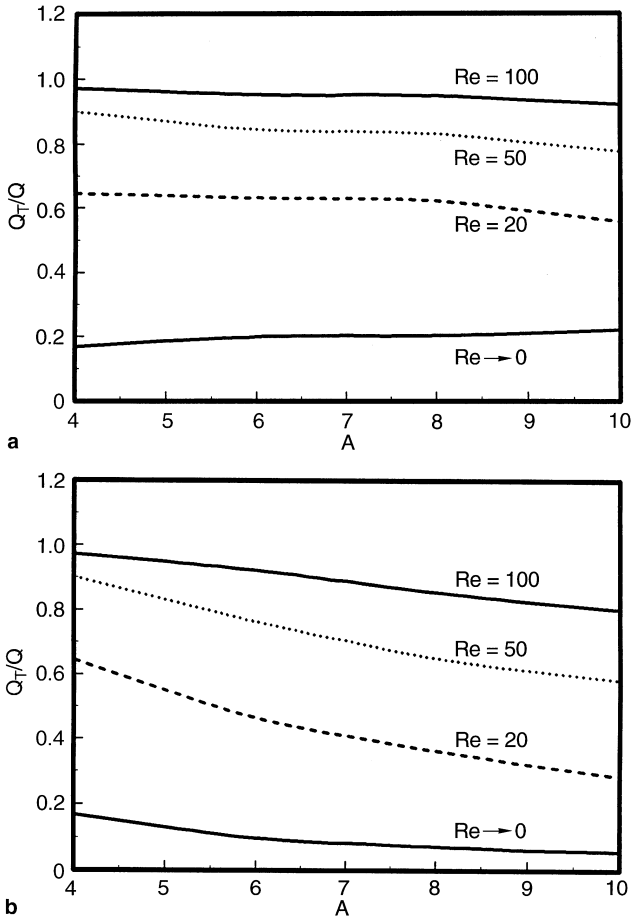

Fig. 5a,b. Entrance and exit length effect on the heat transfer through the top, Q_T/Q, for natural and mixed convection with $\mathrm{Ra} = 10^6$ and various Re numbers. **a** Entrance length effect; **b** Exit length effect

The variation of dimensionless temperature as a function of the Reynolds number for entrance and exit lengths of 4, 6 and 10 is shown in Fig. 6a and b respectively. Figure 6a shows the entrance length effect: the temperature on the electronic components increases when the entrance length varies from $A = 4$ to 6 and then decreases when A varies from 6 to 10. The variation of temperature on the electronic components with the Reynolds number is similar to that observed earlier in Fig. 4. It is seen that the entrance effect is more pronounced for natural convection and at low Reynolds numbers. For high Reynolds numbers, there is no discernible effect. It is seen that θ goes through a maximum for $A = 6$. A cross plot of the data showed that θ had, in fact, a maximum at about $A = 6$ for

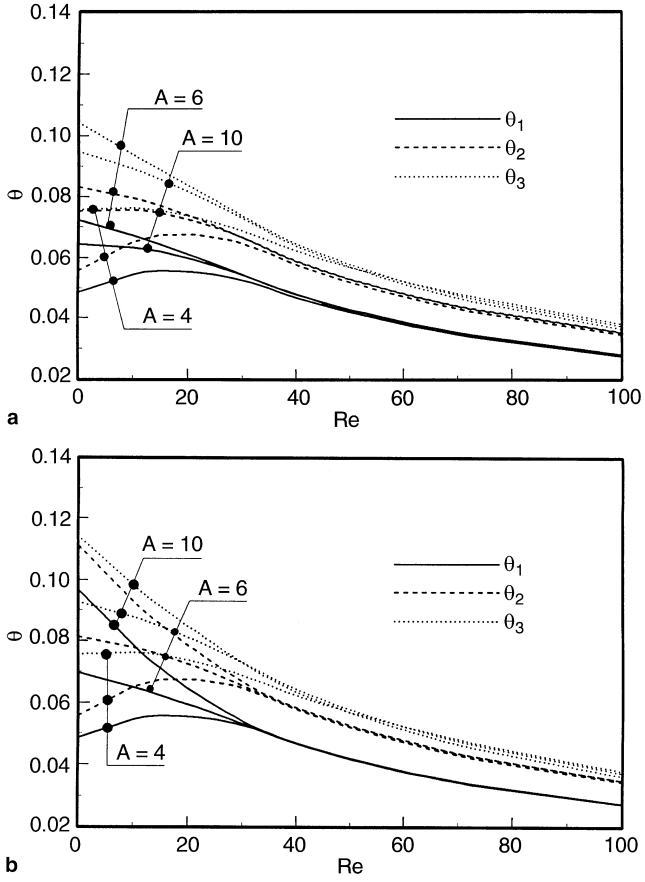

Fig. 6a,b. Temperature at the electronic components as a function of Reynolds number with $\mathrm{Ra} = 10^6$ for various aspect ratios, A. **a** Entrance length effect on temperatures θ_i at the electronic components ($i = 1, 2, 3$) as a function of the Reynolds number for $\mathrm{Ra} = 10^6$, **b** Exit length effect on temperatures θ_i at the electronic components ($i = 1, 2, 3$) as a function of the Reynolds number for $\mathrm{Ra} = 10^6$

all three cases at low Reynolds numbers. An examination of the streamlines and isotherms showed that the circulation in the channel decreased with increasing entrance length up to 6 and then increased slightly. As a result, the cooling of the components was least effective at $A \approx 6$. The variation of temperature in Fig. 6(b) for the exit length effect has a similar trend, except the temperature variation is an increasing function of the exit length at low Reynolds numbers. However, a cross plot of the data for this case also showed that θ was going through a maximum, this time at $A \approx 8$. The reason for these maxima was similar to that for the entrance effect. Again, the exit length effect is more pronounced for natural convection and at low Reynolds numbers. Figure 6 shows that an extension of the channel at the entrance or exit from the electronic components does not have a beneficial effect on cooling of these components at low Reynolds numbers and there is no discernible effect at high Reynolds numbers.

The effect of the positions of the electronic components has been studied by changing their order from 1, 2, 3 (case A; base case) to 1, 3, 2 (case B) and 3, 2, 1 (case C). It was observed that the thickest component blocking the channel is the third component and the thinnest, blocking it the least is the second. Thus, the position of the thickest component, no. 3, has been changed from the top to the middle and to the bottom to see its influence on the heat transfer and temperature distributions. It should be noted however that heat generated uniformly in each component is S, and based on Table 1, the power in the component no. 1 is the highest followed by the third with about 60% of the first and then the second with 33% of the first. Hence, a trade off is expected between the influence of the power generated in a component and the blockage of the channel to flow for different cases. The results for natural convection and mixed convection showed (not presented in figures) that the most effective cooling was always at the component placed at the entrance, followed by that at the middle position and finally least effective cooling was at the top position. This trend seems to be independent of the component size.

5 Conclusions

It is found that the heat transfer from the electronic components is affected considerably by the imposed flow, the strength of the natural convection and the aspect ratio. The heat transfer through the top is an increasing function of the imposed flow rate and a decreasing function of the strength of natural convection. It is found that the heat transfer through the right increases with decreasing Re and increasing Ra. The temperatures at the electronic components decrease with increasing Re and increasing Ra when Re is small. At higher Re numbers, the effect of Ra on the temperatures is not big. Parametric studies with aspect ratio showed that the heat transfer through the top is generally a decreasing function of the aspect ratio. However, for small aspect ratio there is an optimum condition where the heat transfer through the top is maximized. Entrance and exit lengths have a negative effect on cooling of components by natural convection and by mixed convection at low Reynolds numbers. By mixed convection at high Reynolds numbers, the influence of entrance and exit lengths is negligibly small. Finally, positioning of the electronic components in the channel is important. Generally, the best cooled component is one placed at the entrance of the channel, regardless of its power dissipation and its size.

References

1. **Incropera FP** (1988) Convection heat transfer in electronic equipment cooling. J. Heat Transfer, 110: 1097–1110
2. **Chen YM; Kuo Y** (1990) Studies on natural convection heat transfer from arrays of block-like heat-generating modules on a vertical plate. Heat Transfer in Electronic and Microelectronic Equipment. edited by A.E.Bergles, Hemisphere Publishing Corp., New York, pp 125–138
3. **Hasnaoui M; Bilgen E; Vasseur P; Robillard L** (1991) Mixed convection heat transfer in a horizontal channel heated periodically from below. Numerical Heat Transfer. Part A 20: 297–315.
4. **Aung W; Chimah B** (1990) Laminar heat transfer exchange in vertical channels application to cooling of electronic systems. Low Reynolds Number Flow Heat Exchangers. edited by S. Kakaç, R.K. Shah and A.E. Bergles, pp 395–413
5. **Bergles AE** (ed.) (1990) Heat Transfer in Electronic and Microelectronic Equipment. Hemisphere Publishing Corp., New York

6. **De Almeida PIF; Milanez LF** (1990) Laminar mixed convection between vertical plates with isolated thermal sources. Heat Transfer in Electronic and Microelectronic Equipment. edited by A.E. Bergles, Hemisphere Publishing Corp., New York, pp 155–168
7. **Jaluria Y** (1986) Mixed convection flow over localized multiple thermal sources on a surface. Phys. Fluids 29: 934–940
8. **Show H-J; Chen C-K; Cleaver JW** (1990) Mixed convective heat transfer in vertical cavities with heated bottom surface. Heat Transfer in Electronic and Microelectronic Equipment, edited by A.E. Bergles, Hemisphere Publishing Corp., New York, pp 169–183
9. **Tanda G** (1988) Natural convection in partially heated vertical channels. Wärme-und Stoffübertragung 23: 307–312
10. **Yan WM; Lin TF** (1987) Natural convection heat transfer in vertical open channel flows with discrete heating. Int. Comm. Heat Mass Transfer 14: 187–200.
11. **Webb BW; Hill DP** (1989) High Rayleigh Number laminar natural convection in an asymmetrically heated vertical channel. J. Heat Transfer 111: 649–656
12. **Yücel C; Hasnaoui M; Robillard L; Bilgen E** (1993) Mixed convection heat transfer in open ended inclined channels with discrete isothermal heating. Num. Heat Transfer Part A 23: 45–63
13. **Keyhani M; Chen L** (1991) The aspect ratio effect on natural convection in an enclosure with protruding heat sources. J. Heat Transfer 113: 883–891
14. **Park KA; Bergles AE** (1987) Natural convection heat characteristics of simulated microelectronic chips. J. Heat Transfer 109: 90-96
15. **Patankar SV** (1980) Numerical Heat Transfer and Fluid Flow. Hemisphere Publishing Corp., New York
16. **Du Z-G; Bilgen E** (1992) Natural convection in vertical cavities with internal heat generating porous medium. Wärme- und Stoffübertragung 27: 149–155